Virology 404 (2010) 41–50

Contents lists available at ScienceDirect

Virology

journal homepage: www.elsevier.com/locate/yviro

Protein binding sites involved in the assembly of the KplE1 prophage intasome

Gaël Panis [a,b], Yohann Duverger [a], Stéphanie Champ [a], Mireille Ansaldi [a,b,*]

[a] Laboratoire de Chimie Bactérienne CNRS UPR9043, Institut de Microbiologie de la Méditerranée, Marseille, France
[b] Aix-Marseille Université, Marseille, France

ARTICLE INFO

Article history:
Received 25 January 2010
Returned to author for revision
24 February 2010
Accepted 27 April 2010
Available online 21 May 2010

Keywords:
Bacteriophage
Prophage
Site-specific recombination
Prophage excision
Intasome
Recombination directionality factor
Integrase

ABSTRACT

The organization of the recombination regions of the KplE1 prophage in *Escherichia coli* K12 differs from that observed in the λ prophage. Indeed, the binding sites characterized for the IntS integrase, the TorI recombination directionality factor (RDF) and the integration host factor (IHF) vary in number, spacing and orientation on the *att*L and *att*R regions. In this paper, we performed site-directed mutagenesis of the recombination sites to decipher if all sites are essential for the site-specific recombination reaction and how the KplE1 intasome is assembled. We also show that TorI and IntS form oligomers that are stabilized in the presence of their target DNA. Moreover, we found that IHF is the only nucleoid associated protein (NAP) involved in KplE1 recombination, although it is dispensable. This is consistent with the presence of only one functional IHF site on *att*R and none on *att*L.

Introduction

Site-specific recombination, which involves tyrosine or serine recombinases, mediates chromosome integration and excision in temperate bacteriophages (Argos et al., 1986; Smith and Thorpe, 2002; Nunes-Duby et al., 1998). In phage λ, the most studied model, both integration and excision reactions are performed by the Int integrase that belongs to the well characterized family of tyrosine recombinases (Nunes-Duby et al., 1998). This family includes λ type integrases, resolvases, invertases and transposases. These categories show little homology at the protein level excepted in their C-terminal domains, which constitute the catalytic domains (Nunes-Duby et al., 1998). The Int protein of phage λ is a tyrosine recombinase consisting of 356 amino-acids which binds to DNA in a heterobivalent manner involving two different domains of the protein. The core-binding domain which comprises amino-acids 70 to 169 is part of the C-terminal domain and binds with low affinity the core sites (*O* sites) where the recombination reaction occurs (Tirumalai et al., 1997; Tirumalai et al., 1998; Kovach et al., 2002). This interaction enables the catalytic domain (residues 170 to 356) to come into close proximity with the core sites (Kamadurai and Foster, 2007). The small N-terminal domain (residues 1 to 70) binds arm-type sites (*P* and *P′* sites) with high affinity (Lee et al., 2005; Radman-Livaja et al., 2006; Fadeev et al., 2009). This domain also permits protein oligomerization, which is essential for the intasome formation (Jessop et al., 2000). However, despite its intrinsic DNA binding properties, Int is not able to mediate the formation of a fully assembled intasome by itself and requires the assistance of several accessory proteins. The Xis protein is required for excisive recombination, directing Int-mediated recombination towards excision and inhibiting reintegration (Gottesman and Abremski, 1980; Abremski and Gottesman, 1981; Sam et al., 2002). Xis acts as a recombination directionality factor (RDF) as it bears no catalytic activity but rather directs the Int driven reaction towards excision (Lewis and Hatfull, 2001). It plays an architectural role in the formation of the excisive intasome by binding and bending DNA, and prevents reintegration of the excised phage genome (Miller and Friedman, 1980; Abremski and Gottesman, 1982; Numrych et al., 1992). Other accessory proteins are host-encoded and are members of the nucleoid associated protein family (NAP) such as IHF, Fis and HU. The main player, IHF is required for both integration and excision reactions and recognizes three different sites on the recombination regions (Nash and Robertson, 1981; Gardner and Nash, 1986; Thompson et al., 1986). IHF has a strong ability to bend DNA which promotes juxtaposition of the Int arm-type and core-type binding sites (Rice et al., 1996). However, in the absence of IHF, either the HU protein that also bends DNA or bending-prone DNA sequences are sufficient *in vitro* to restore recombination (Goodman et al., 1992; Goodman and Kay, 1999). If Xis can be considered as the major

Abbreviations: RDF, recombination directionality factor; Int, integrase; IHF, integration host factor; Xis, excisionase; NAP, nucleoid associated proteins; LB, Luria broth; CFU, colony forming unit; IPTG, isopropyl β-D-thiogalactopyranoside; AU, arbitrary unit(s).

* Corresponding author. Laboratoire de Chimie Bactérienne, IMM-CNRS, 31 chemin Joseph Aiguier, 13402 Marseille Cedex 20, France. Fax: +33 4 91 71 89 14.
E-mail address: ansaldi@ifr88.cnrs-mrs.fr (M. Ansaldi).

0042-6822/$ – see front matter © 2010 Elsevier Inc. All rights reserved.
doi:10.1016/j.virol.2010.04.027

determinant controlling directionality, and assembly of Xis nucleoprotein filament is facilitated by the cooperative binding of Fis (Papagiannis et al., 2007).

The KplE1 prophage (also named CPS-53) contains 16 open reading frames and is one of the 10 prophage remnants present in *E. coli* K12 MG1655 (Rudd, 1999; Casjens, 2003). Although KplE1 is highly defective, it is fully competent for site-specific recombination (ElAntak et al., 2005; Panis et al., 2007). The recombination sites are composed of 16 bp-duplicated core sequences (CTGCAGGGGACACCAT) separated by 10.216 kb bordered by the *argW* tRNA gene and the *dsdC* gene. Previous work identified the recombination protein binding sites of KplE1 and they were highly similar to that of Sf6 and HK620 phages, as well as strains K1 RS218, UTI89, APEC-O1 and SsO46 prophages (Casjens et al., 2004; Clark et al., 2001; King et al., 2007; Panis et al., 2007). All these phages and prophages target a common attachment site, the *argW* tRNA which is conserved on their host genomes. Therefore a family of site-specific recombination modules was defined. A module is composed of the integrase and excisionase genes and the recombination DNA sequences *att*L and *att*R. This module is related to λ's as it contains binding sites for the integrase (arm- and core-type), the RDF and IHF; however, the number, spacing and orientation of these sites are specific to this module ((Panis et al., 2007) and Fig. 1). In this work, we analyzed the essentiality of the recombination protein binding sites in integrative and excisive recombination reactions. By combining *in vitro* recombination assays to bandshift experiments, we propose a model for the KplE1 excisive intasome assembly.

Results and discussion

IHF is the major nucleoid associated protein involved in KplE1 site-specific recombination

Previous results showed that IHF was dispensable for KplE1 recombination *in vitro* although its presence increased the efficiency of the reaction (Panis et al., 2007). We therefore asked the question of whether another nucleoid associated protein (NAP) present in *E. coli* K12, such as HU, H-NS and Fis, and described to favor recombination in other systems (Numrych et al., 1991; Goodman et al., 1992; Shiga et al., 2001; Papagiannis et al., 2007) could compensate for the non-essentiality of IHF in KplE1 recombination. To answer this question, we performed *in vivo* excision assays as previously described (Panis et al., 2007). The Kan cassette from several NAP mutants from the KEIO collection (Baba et al., 2006) was removed by using the *flp* encoding plasmid (Datsenko and Wanner, 2000) before transducing back the Kan cassette associated with the KplE1 prophage (LCB984) (see Materials and methods). These strains were then transformed with the pJFi plasmid that allowed the production of the TorI RDF upon addition of IPTG. In a wild-type context, the Ap^R/Km^R ratio was about 340, meaning that, in these conditions, the expression of TorI resulted in a 340 fold increase in excision (Fig. 2). As a control, we used an *ihfA* strain, and we observed a decreased excision rate consistent with the involvement of IHF in KplE1 site-specific recombination. It should be noted that the effect of this mutation is much less than that for λ

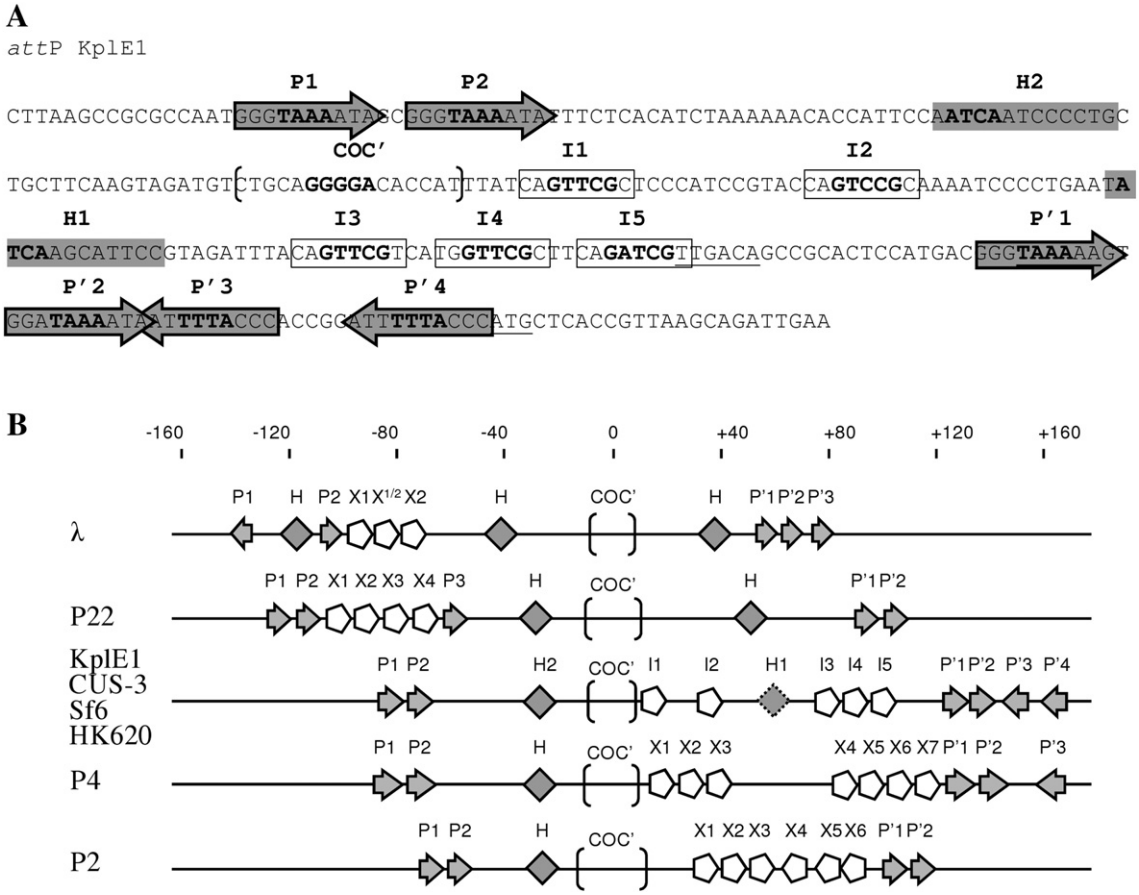

Fig. 1. Overview of the KplE1 recombination module. (A) The nucleotide sequence of the *att*P DNA substrate used in this study is indicated. IntS arm-type sites (*P* and *P′*) are represented by a grey arrow, TorI sites (I) are boxed, IHF sites (H) are highlighted in grey and the core sequence is framed by brackets (COC′). Nucleotides that were changed for the complement are shown in bold (see Materials and methods). (B) Schematic overviews of the *att*P regions of different phages are represented. To facilitate comparison, numbering is relative to the centre of the core sequence to serve as an identical reference in all *att*P sequences. Protein binding sites are represented as follows: Integrase core-type, brackets; Integrase arm-type, grey arrows; RDF, pentagons; IHF, grey diamonds.

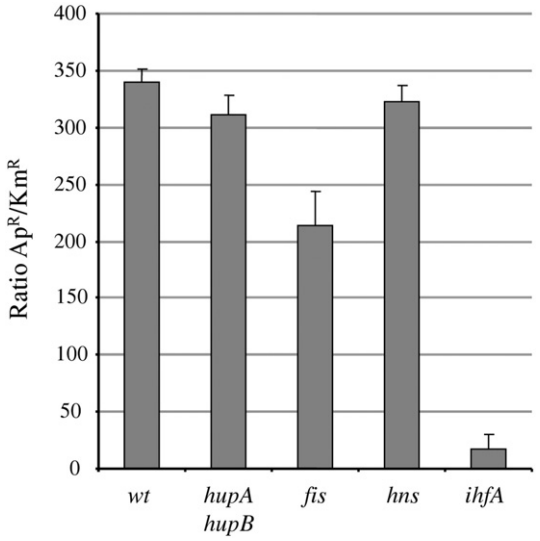

Fig. 2. IHF is the major nucleoid associated protein involved in KplE1 excision *in vivo*. Ratios of ampicillin-resistant over kanamycin-resistant colonies were measured in various genetic backgrounds. Strains LCB984 (wild-type), LCB6022 (*hupA hupB*), LCB6023 (*hns*), LCB6027 (*fis*), and LCB6028 (*ihfA*) were transformed with pJFi (Ap^R) and *in vivo* excision assay was performed as described in Materials and methods. Experiments were carried out in triplicate and repeated at least twice, standard deviations are indicated.

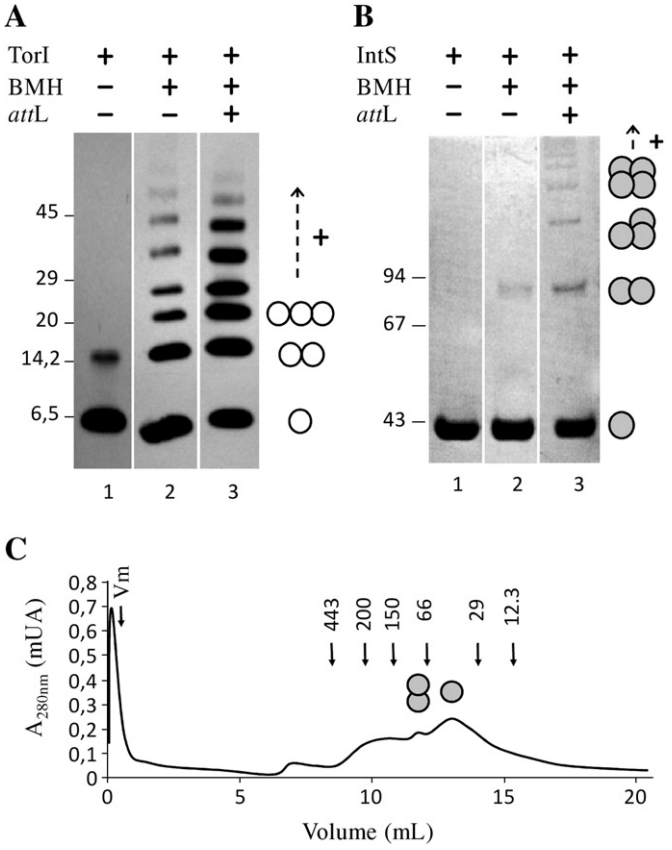

Fig. 3. Oligomerization of TorI and IntS. The oligomerization properties of TorI and IntS in solution were analyzed by SDS PAGE in the presence or absence of BMH as a cross-linking agent and in the presence or absence of the *att*L DNA region (A, B). (A) Purified TorI (100 μM) revealed with α-TorI antiserum. (B) Purified IntS (20 μM) revealed with Coomassie blue. (C) IntS oligomerization was analyzed by size exclusion chromatography.

recombination (Miller and Friedman, 1980; Miller et al., 1980). In contrast to *ihfA*, in the *hupA hupB* and *hns* genetic backgrounds, we measured a similar ratio to what in the wild-type strain, indicating that HU and H-NS have no role in this reaction. A 30% decrease of excision efficiency was observed in the *fis* background compared to the wild-type; however the excision efficiency remained high compared to that observed with the *ihfA* mutation. Compared to phage λ excision NAP requirements, we noticed that *fis* was dispensable in KplE1, whereas the *fis* mutant leads to a 200-fold decrease in λ excision (Ball and Johnson, 1991), and the *ihfA* mutant, although it led to a 20-fold decreased in KplE1 excision, has a more dramatic effect on λ excision where a 500- to 5000-fold decrease is described in the absence of IHF (Cho et al., 1999). Altogether, these results show that IHF is the major nucleoid associated protein involved in KplE1 recombination although it proved to be non-essential *in vitro* as well as *in vivo*.

IntS and TorI form oligomers stabilized in the presence of target DNA

To better understand the KplE1 intasome assembly, we first analyzed the oligomerization of IntS and TorI in the presence or absence of target DNA. Purified proteins were incubated in the presence or absence of BMH as a cross-linking agent and/or *att*L DNA. Proteins were then denaturated and separated using a SDS tricine-PAGE (Fig. 3). In the absence of BMH, the TorI protein was mainly present as a monomer although a stable dimeric form was also observed (Fig. 3A, lane 1). This is consistent with native gel analysis and crystallographic results (data not shown and (Huang et al., 2007)). Upon addition of 1 mM BMH, several multimeric forms of TorI were stabilized ranging from a size corresponding to dimeric forms up to very high molecular weight oligomeric forms (Fig. 3A, lane 2), indicating that TorI has the ability to form high molecular weight complexes in solution. When *att*L was incubated with TorI and BMH, the higher forms of TorI were stabilized whereas BMH did not crosslink DNA, revealing an influence of the target DNA on the multimerisation of TorI. The same experiment was performed using the IntS protein (Fig. 3B), which was exclusively present as a monomer under denaturing conditions. Nevertheless, when loaded onto a size exclusion chromatography column, high molecular weight forms of IntS were observed although the major peak corresponded to a monomeric form (Fig. 3C). Under denaturing conditions and in the presence of BMH, a slight band with an apparent molecular weight consistent with a dimer of IntS was observed, which abundance increased in the presence of *att*L (Fig. 3B). Moreover, several additional forms of high molecular weight were detected. Therefore, as shown for TorI, IntS is able to form oligomers that are stabilized in the presence of the target DNA.

Site-directed mutagenesis of the recombination binding sites

To further characterize the recombination sites involved in the intasome formation, and therefore in the recombination reactions, we performed site-directed mutagenesis. For IntS and TorI binding sites, we decided to change the central four (IntS arm-type) or five (IntS core sequence and TorI binding sites) nucleotides of each conserved motif by its complementary sequence (Fig. 1). In the case of IHF we changed the four most conserved nucleotides at the beginning of the consensus sequence. All IntS binding sites (arm-type sites and core sequence) were mutated independently whereas we decided to mutagenize the TorI binding sites in two blocks, one consisting of the *I1* and *I2* sites and the second comprising *I3* to *I5* (Fig. 1). Mutations were performed either directly, by using one mutagenic primer, or in two steps depending on the location of the mutation (see Materials and methods).

Involvement of the recombination sites in site-specific recombination in vitro

In vitro excision and integration assays were performed essentially as previously described (Panis et al., 2007). A few improvements were made to the original method such as lowering the IHF concentration to reach an IHF:IntS protein ratio of 1:3 (compared to 1:1) that allowed a higher efficiency on linear substrates (data not shown) consistent with the IHF inhibitory effect in λ excisive recombination (Thompson et al., 1986). We performed all assays with PCR-amplified linear substrates, wild-type and mutants. Figs. 4 and 5 show the results obtained in excisive and integrative recombination assays, respectively. Negative controls used substrates containing a mutated core sequence in *att*L, *att*R, and *att*P. When used in the quantitative *in vitro* assay these substrates achieved a complete inactivation of the reaction in either direction (Figs. 4 and 5). In case IntS would bind to this mutated core, we checked if a compensatory mutation on the second substrate would allow recovering some activity. We thus used core mutated *att*L and *att*R in excisive recombination, and as indicated in Fig. 4, no recovery was observed. Regarding the excisive recombination reaction, one could classify these substrates into three categories: (i) mutated substrates that behave similarly to wild-type DNA, allowing to reach a 50 to 80% efficiency (*H1** and *P′3**), (ii) substrates leading to a drastic decrease of the reaction efficiency, less than 10% (*I1*I2**, *I3*I4*I5**, *P′1** and *P2**), and (iii) substrates with intermediate behavior, 10 to 30% efficiency (*P′2**, *P′4**, *P1** and *H2**). Together, these results reveal that the IntS arm-type sites are not equivalent although they are made of the same sequence. *P′3* is the most dispensable, and interestingly this site is absent (or too degenerated to be detected) in the corresponding *att*L region of the P4 satellite phage, which shows the closest organization with KplE1 (Panis et al., 2007). *P′1* and *P2*, located on *att*L and *att*R respectively (Fig. 1), are the most essential sites, whereas the four remaining sites show an intermediate phenotype when mutated. Regarding TorI, the two blocks of sites are essential for the excisive reaction to occur, thus confirming the essential role played by the RDF protein in the excisive recombination reaction. Out of the two IHF sites identified, only the one present on *att*R (*H2*), and the closest to the consensus sequence with only one mismatch, seemed to be involved in the excisive recombination. Interestingly, this site was present on the recombination substrate where no TorI site was found (Fig. 1).

When performing *in vitro* integrative recombination in the absence of the TorI protein, the maximum efficiency reached was about 16% of substrates transformed into products (Fig. 5). We previously obtained lower efficiencies with linear substrates and we found that lowering the IHF concentration was improving the reaction ((Panis et al., 2007) and data not shown) which was not observed in λ integrative recombination. Interestingly, the same sites that we found dispensable for the excisive recombination, namely *P′3* and *H1*, appeared to be non-essential in integrative recombination. As

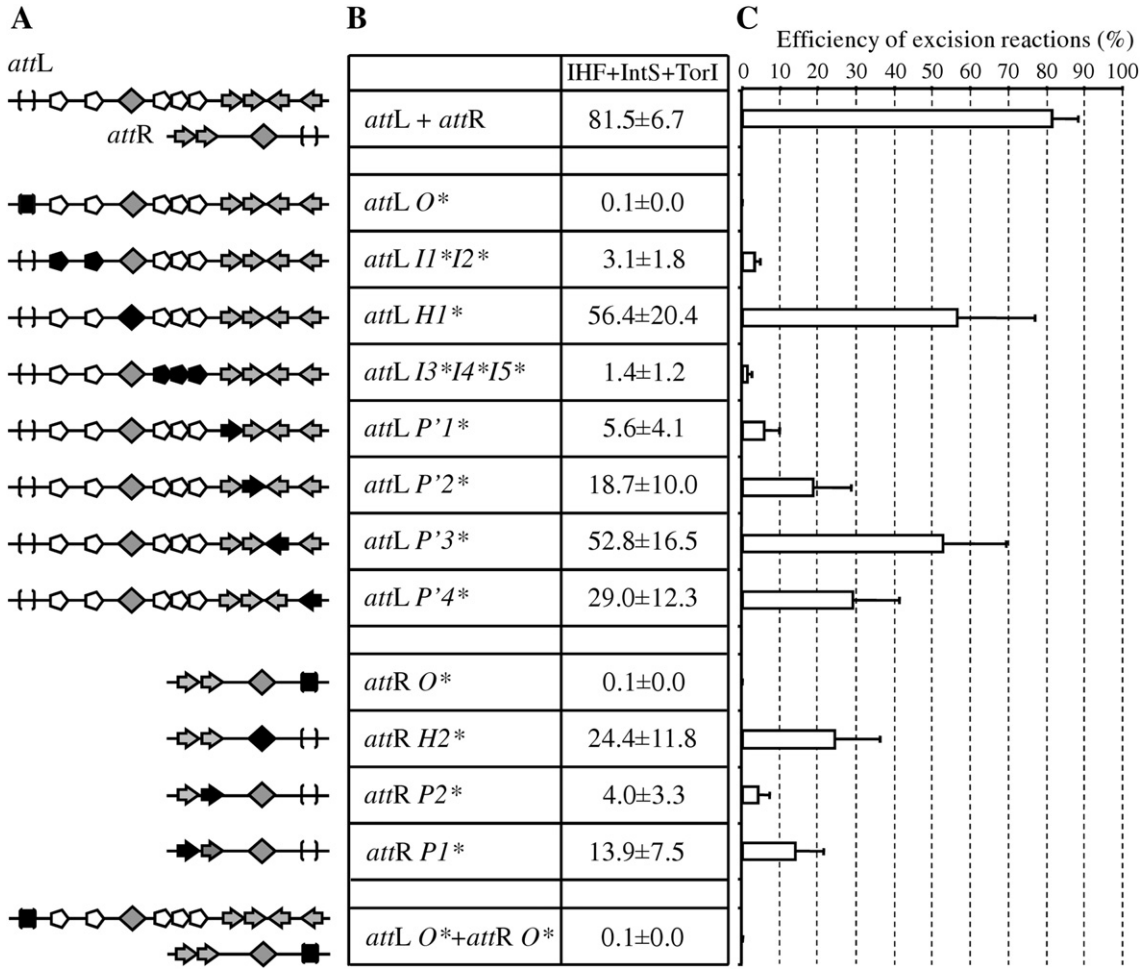

Fig. 4. Effect of protein binding site mutations on excisive recombination. (A) Schematic representation of the linear *att*L and *att*R substrates used in this assay. Symbols for protein binding sites are identical as in Fig. 1B. Mutations of these sites are mentioned by a black colouring of the respective symbols. For convenience, only mutated substrates are indicated. (B) Excisive recombination was performed as described in Materials and methods. The amount of substrate transformed into *att*P was quantified by real-time PCR and the excision efficiency is expressed as the percentage of the substrates transformed into products. Values represent the averages of four independent experiments, standard deviations are indicated. (C) Recombination efficiencies shown in (B) are represented as histogram bars.

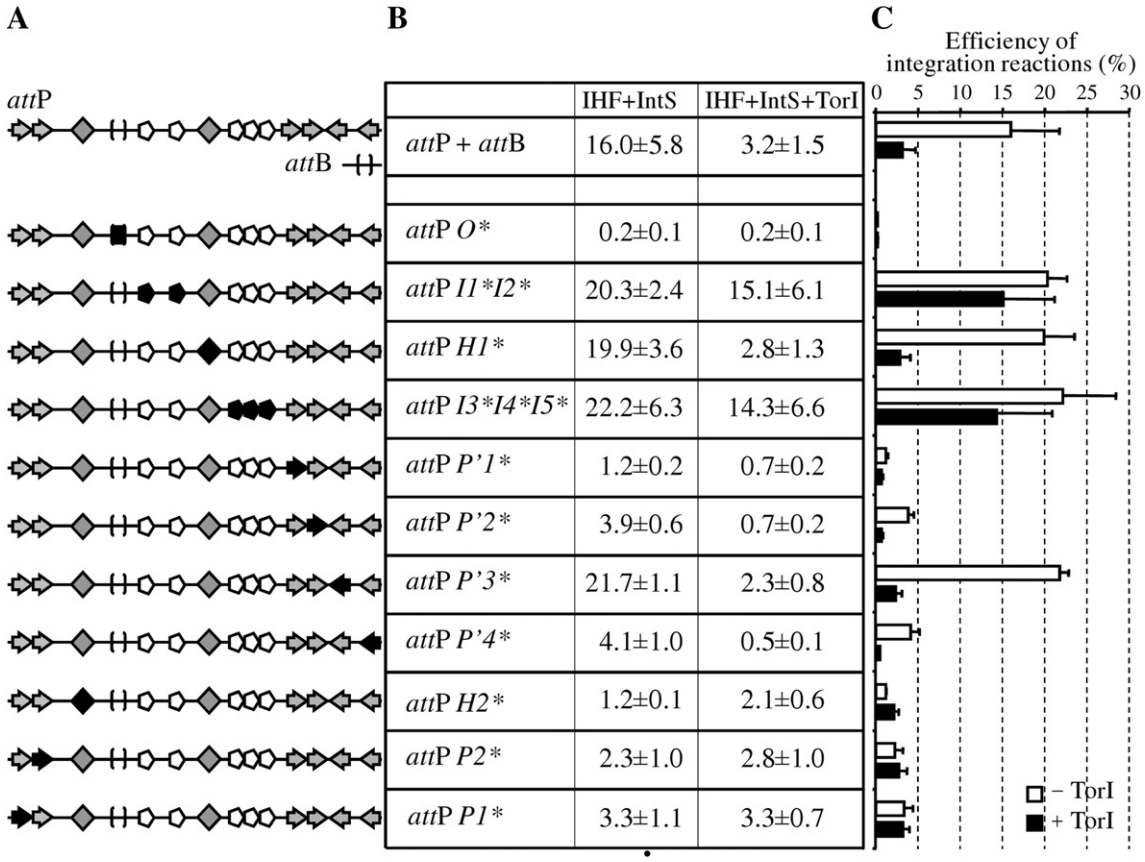

Fig. 5. Effect of protein binding site mutations on integrative recombination. (A) Schematic representation of the linear *att*P and *att*B substrates used in this assay. Symbols for protein binding sites are identical as in Fig. 1B. Mutations of these sites are mentioned by a black colouring of the respective symbols. For convenience, only mutated substrates are indicated. (B) Integrative recombination was performed as described in Materials and methods in the presence or absence of TorI as indicated. The amount of substrate transformed into *att*R was quantified by real-time PCR and the integration efficiencies are expressed as the percentage of the substrates transformed into products. Values represent the averages of four independent experiments, standard deviations are indicated. (C) Results shown in (B) are represented as histogram bars (−TorI, white bars; +TorI, black bars).

expected, mutations in the TorI sites did not affect the reaction in the absence of TorI (Fig. 5). Mutations in all remaining sites (*P′1*, *P′2*, *P′4*, *H2*, *P1* and *P2*) severely affected the efficiency of the integrative recombination. As before the *P′1* site appears to be the most important arm-type site since its mutation led to a 15 to 20 fold decrease in efficiency. In contrast to the excisive recombination, a mutation in the IHF site present on *att*R (*H2*) resulted in a substantial decrease in the reaction efficiency similar to that seen for the *P′1* mutation (Fig. 5). Thus, the role of IHF appears more important in the integrative than in the excisive recombination. Upon addition of TorI, the integrative reaction efficiency dropped 5 to 7 fold (Fig. 5), consistent with the inhibitory role of the RDF proteins in integrative recombination. When either block of TorI sites was mutated, the inhibition was released, although the efficiency did not reach the same level as in the absence of TorI (Fig. 5). These data suggest that both blocks of TorI sites are involved in the inhibition mechanism albeit one of these is not sufficient to carry out complete inhibition.

Looking into the KplE1 intasome assembly: characterization of IntS and TorI DNA binding on attL and attR

Our previous work used DNAse protection experiments to study the recombination protein binding sites (Panis et al., 2007). In order to depict the different steps that lead to the intasome assembly, we carried out bandshift experiments with IntS and TorI proteins, using wild-type as well as various mutated DNA (Material and methods). On the *att*R DNA substrate, the integrase was able to form four different complexes, which was consistent with the presence of several binding sites, two arm-types and one core-type (Fig. 6A). However, this constituted an unusual profile as the number of complexes observed is larger than the number of integrase binding sites. Changing five nucleotides in the centre of the core-type sequence, which had a drastic effect on recombination (Fig. 4B), did not modify the profile of the shifted DNA (Fig. 6B), suggesting that the profile observed with the wild-type DNA was only due to IntS arm-type binding. Therefore, this complex pattern probably reflects some rearrangement in the association of IntS to DNA. One possible explanation would be that the binding of a dimer of IntS promotes a conformational change of the DNA, which in turn favors the association of a tetramer. A mutation in either *P1* or *P2* dramatically affected IntS binding to *att*R (Figs. 6C and D). Indeed, only one complex that showed a long range migration still appeared and for higher IntS concentrations than necessary to shift the wild-type DNA (0.3 compared to 1.2 μM). As mutation of the *P2* site had the most drastic effect, we propose that *P2* might be the primary binding site for IntS. This result is consistent with the fact that in the *in vitro* excision assay the *att*L *P2** substrate led to a lower efficiency that the *P1** DNA (Fig. 4). DNA mutated on the three IntS sites was used as a control and showed no shift in the presence of IntS (Fig. 6E). This last result is consistent with *P1* and *P2* being responsible for all the shifted forms.

On *att*L DNA (Figs. 6F–M), the profile observed in the presence of increasing amounts of IntS is surprisingly less complex than on *att*R. In fact, only three different complexes were observed while four arm-type and one core-type binding sites are present on *att*L (Fig. 6J). It is thus probable that IntS binding occurred in two major steps where an IntS dimer binds first, then favors a second dimer binding, which in turn

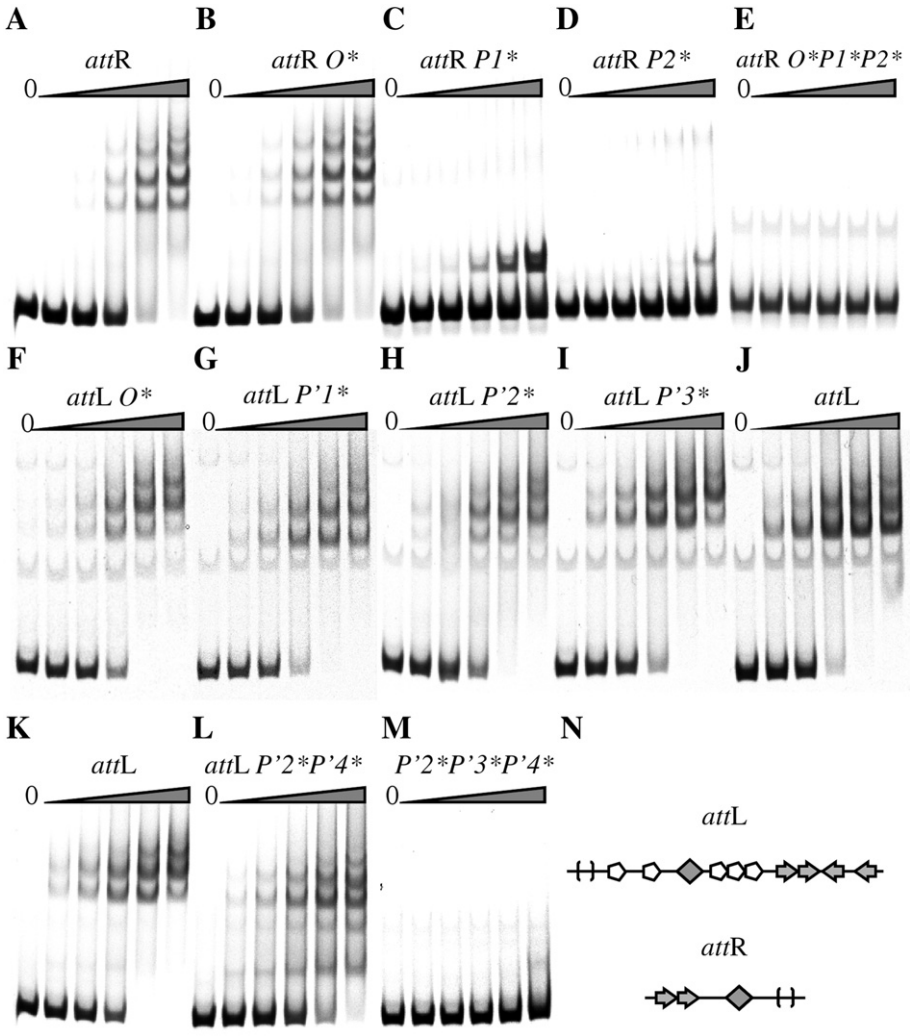

Fig. 6. IntS binding to *att*L and *att*R. Cy5-*att* fragments (*att*R, 135 bp; *att*L, 222 bp), wild-type and mutants, were incubated with increasing concentrations of IntS (0.075, 0.15, 0.3, 0.6 and 1.2 μM) and run on a 4% native PAGE. (A), wild-type *att*R; (B), *att*R *O**; (C), *att*R *P1**; (D), *att*R *P2**; (E), *att*R *O*P1*P2**; (F), *att*L *O**; (G), *att*L *P′1**; (H), *att*L *P′2**; (I), *att*L *P′3**; (J, K), wild-type *att*L; (L), *att*L *P′2*P′4**; (M), *att*L *P′2*P′3*P′4**; (N), schematic representation of *att*L and *att*R substrates. Symbols are identical as in Fig. 1B.

promotes the rearrangement of the whole nucleoprotein complex. This idea was favored by the fact that none of the individual arm-type site mutation led to a change in the retardation profile (Figs. 6G–J). At the most, we observed a difference in the relative migration of the fastest running complex for the *P′3** mutation (Fig. 6I), which had barely no effect on recombination (Fig. 4). When the *P′2** and *P′4** mutations were combined, the migration profile did not change much except for the appearance of two discrete bands that run faster (Fig. 6L). The fastest running form was the only remaining, and appears only at high integrase concentrations, when the *P′3* mutation was added to the former two (Fig. 6M). *P′2* and *P′4* belong to the four-fold arm-type motif and are in opposite orientation (Fig. 1). Therefore, changing only one site of a direct repeat still enabled the binding of an IntS dimer. Surprisingly, the *P′3** mutation, added to the former two, abolished IntS binding although this site proved to be non-essential in the recombination assay (Fig. 4). Therefore, *P′3* can have an important structural role in the absence of other binding sites.

Regarding TorI binding to *att*L we observed a particular DNA retardation profile. Indeed, whereas five TorI binding sites were identified on this part of the recombination region, only one stable complex was formed (Fig. 7A). Moreover, at intermediate protein concentrations (1.5 to 3 μM), no transitional complex could be

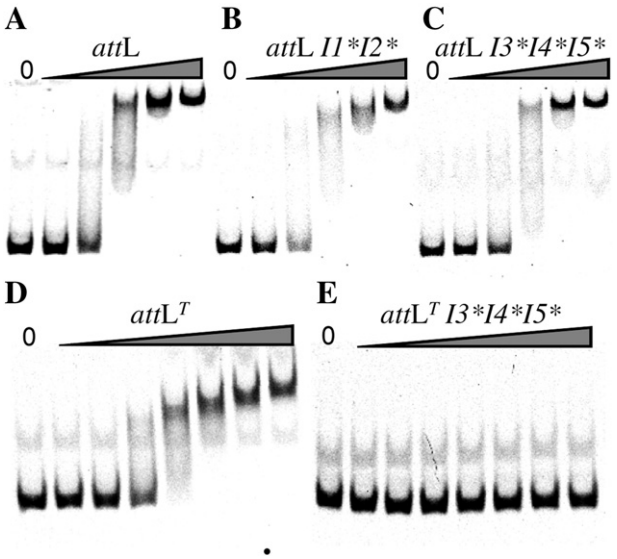

Fig. 7. TorI binding to *att*L. Cy5-*att*L fragments (*att*L, 222 bp, I1, I2, I3, I4, I5; *attL*^{T}, 167 bp, I3, I4, I5), wild-type and mutants, were incubated with increasing concentrations of TorI ((A–C) 0.75, 1.5, 3, 6 and 12 μM, (D–E) 0.34, 0.69, 1.4, 2.75, 5.5, 11, and 22 μM) and separated on a 4% native PAGE. (A), wild-type *attL*; (B), *attL I1*I2**; (C), *attL I3*I4*I5**; (D), *attL*^{T}; (E), *attL*^{T}*I3*I4*I5**.

observed but rather a smearing shift that eventually resumed to a single, well defined, shift at a higher protein concentration (6 μM). A similar profile was observed with Cox proteins, that have RDF function, in P2 and other related phages (Ahlgren-Berg et al., 2009). Thus, either TorI has the same affinity for all five binding sites or TorI binding is highly cooperative and binding to a primary entry site then allows binding on the adjacent sites. To decipher between these two assumptions, we used DNA substrates that lack either one of the two blocks of TorI binding sites. Surprisingly, we obtained a wild-type profile with both substrates (Figs. 7B and C), indicating that one block is sufficient to allow the formation of a full TorI–*att*L complex. We then checked that the mutations did actually prevent TorI binding as suggested by the dramatic effect these mutations had on the efficiency of site-specific recombination (Fig. 4). Rather than combining mutations, we used a truncated *att*L substrate that contained only the second TorI block (*att*L^T). In the presence of *att*L^T DNA, the retardation profile, except for the distance run, was similar to that obtained with the full length *att*L: no shift at a low protein concentration, a smearing shift at intermediate concentrations, and finally a single stabilized complex whereas three binding sites were still present (Fig. 7D). As expected, no shift was observed when all three sites in block two were mutated (Fig. 7E). As a result, the changes we made in the *I* sites are preventing TorI binding. Together, these results suggest that TorI binding to either one of the two blocks allows the nucleation of the protein to the other block of sites, which induces a strong bending of that DNA region. However this nucleation is not sufficient to allow the excisive recombination to occur (Fig. 4). One explanation is that the TorI complexes formed with the mutated substrates are either unstable or unable to position the integrase correctly.

Assembly of the KplE1 intasome for excisive recombination

The excisive intasome assembly requires long range interactions between two distant core sequences (Fig. 1). In KplE1, pre-intasome assembly on *att*R probably starts with the binding of an IntS monomer on the *P2* site, then on the *P1* site. Although IntS seems to have a higher affinity for *P2* than for *P1*, both sites are essential for the formation of a high molecular weight complex (Figs. 6A–E) and for integrative as well as excisive *in vitro* recombination (Figs. 4 and 5). Mutation in the core site showed no effect on the formation of this complex although this site proved to be protected in a DNAse protection assay (Panis et al., 2007). *P1* and *P2* therefore constitute an entry site that further allows bending of the DNA region and/or stabilizes IntS C-terminal domain binding to the core site. IHF participates in this process by binding to the only IHF site that proved to have an effect *in vitro* (Figs. 4 and 5) and that ideally localized in between the core site and the *P1*, *P2* arm-type sites (Fig. 1B). On the *att*L region the situation is more complex, only *P′3* proved to be dispensable for integrative as well as excisive recombination, however individual mutations of all four *P′* sites did not impair the assembly of a high molecular weight complex on *att*L (Figs. 6F–J). Together with the tandem association and divergent orientation of the four *P′* sites, these results suggest that binding of the integrase to one site of each tandem permits proper binding of a dimer on two adjacent sites. However, excepted for *P′3*, these individual mutations lead to strongly impaired excisive recombination and the retardation profiles only show discrete differences in the distances run by the protein–DNA complexes, indicating either a change of the overall shape of the complex or a defect in the complex stability. As shown in Fig. 4, *P′1* and *P′2* are the most essential sites and probably act as an entry site for the integrase, whereas *P′4*, and to a lesser extend *P′3*, play a positioning and stabilizing role. Regarding TorI, we found that both blocks of RDF sites are strictly essential to direct the recombination reaction towards excision as well as to inhibit integration (Figs. 4 and 5). However, mutated DNA substrates on either block are bound as efficiently as the wild-type by TorI in a highly cooperative manner. Consequently, a single entry site appears sufficient to allow nucleation of the RDF on *att*L. Previous experiments showed that TorI does not nucleate on the DNA sequence in between the two blocks and strongly bends DNA around each block (Panis et al., 2007), whereas nucleation between two Xis sites was observed in λ (Abbani et al., 2007). Considering the propensity of this protein to form multimers, which is reinforced in the presence of DNA (Fig. 3), we propose that TorI binds *att*L as a multimer that allows wrapping of the DNA around it. In the absence of any IHF site, this loop may allow the core sequence to come into close proximity with the arm-type sites bound by IntS. To confirm the further bending of the *att*L region in the presence of TorI and IntS, we performed a footprinting experiment on *att*L with both proteins (Fig. 8). As previously shown, protected regions encompass the core

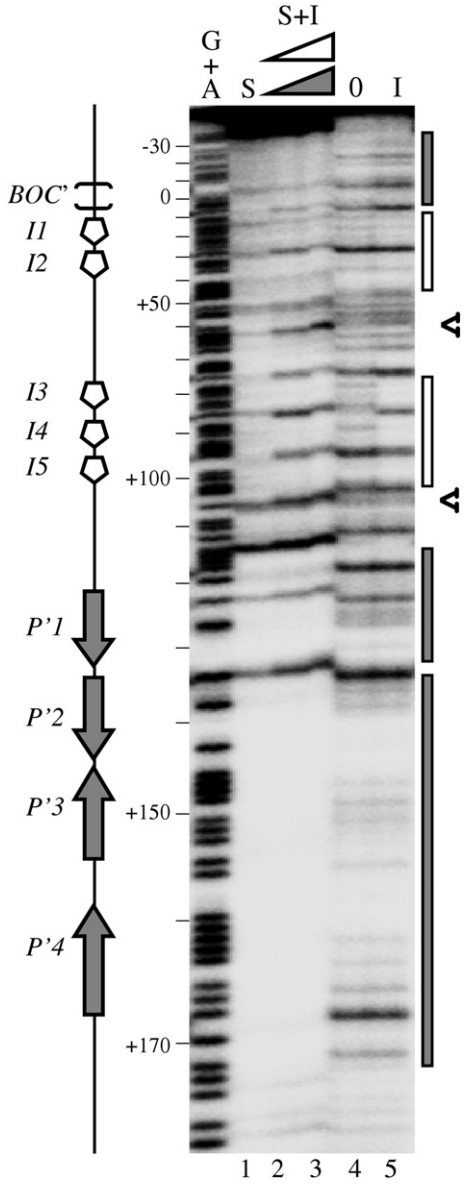

Fig. 8. DNase I footprinting of the KplE1 site *att*L in the presence of both IntS and TorI. 1 nM of a 288-bp labeled DNA fragment encompassing the *att*L region (bottom strand) was digested with DNase I after incubation in the absence (lane 4) or in the presence of purified IntS (lane 1, 0.03 μM), or TorI (lane 5, 0.12 μM) or in the presence of both IntS and TorI (lane 2, 0.015 μM IntS, 0.06 μM TorI; lane 3, 0.03 μM IntS, 0.12 μM TorI). Protected areas by IntS (grey box) and TorI (white box) are indicated. DNase I-hypersensitive sites that appear only in the presence of both proteins are shown (V). G+A sequencing ladders are indicated and numbering is relative to the centre of the core sequence.

and the *P′* sites in the presence of IntS (Fig. 8, lane 1) and all five *I* binding sites in the presence of TorI (Fig. 8, lane 5). It should be noted that for this assay we used lower protein concentrations than previously in order to avoid DNA titration and to be able to identify discrete modifications in the protection profile. Upon addition of both proteins (Fig. 8, lanes 2, 3), we observed a footprint that cumulates the individual prints obtained with individual proteins. Moreover, two hypersensitive sites (positions +62 and +105, indicated by black arrows) appeared only in the presence of both IntS and TorI, indicating that the DNA was further bent than it was with individual proteins. Together these results show that upon binding of TorI and IntS, the *att*L region is strongly bent in between the core sequence and the *P′* sites suggesting that protein binding may allow the core region to come in close proximity with the arm-type sites to proceed to the intasome formation. Based on the number of *I* sites, we assume that TorI would bind as a pentamer, however a structural study would be necessary to fully characterize the TorI–*att*L complex. Eventually, a complete intasome combining the core regions of *att*L and *att*R is assembled, and this final step probably requires the release of four monomers of IntS in order to maintain a single IntS tetramer.

Concluding conjecture

In phage λ, two different asymmetric arrangements have been documented in integrative and excisive complexes based on the interactions between the N-terminal domain of Int and arm-type sites (Biswas et al., 2005; Radman-Livaja et al., 2006; Hazelbaker et al., 2008). The asymmetry in intasome assembly is therefore a major determinant of the reaction directionality in λ site-specific recombination. In KplE1, the *in vitro* excisive and integrative recombination assays that we performed with various mutated substrates suggest that the same combination of IntS arm-type sites is involved in intasome assembly (Figs. 4 and 5). Thus, it is likely that the RDF protein may play a key role in directing the reaction towards excision. This assumption is strengthened by a high number of RDF sites, that induce a strong bending of DNA in the presence of the RDF protein, and located on *att*L upstream of a cluster of arm-type sites. This pattern is overall conserved in P2, P4 and 186 phages where five to seven RDF binding sites are clustered between the core site and the arm-type sites (Yu and Haggard-Ljungquist, 1993; Cali et al., 2004; Frumerie et al., 2005; Panis et al., 2007) (Fig. 1B). It is therefore likely that in these phages, as in KplE1 and other (pro)phages that share the same recombination module, the RDF protein plays a major role in excisive intasome assembly by assisting the binding of the integrase as well as by replacing the NAP benders to a large extend. The satellite phage P4 recombination module presents the closest organization to that of KplE1 and the two *att*P regions share 52% identity. From an evolutionary point of view, it is interesting to note that the P4 sequence does not contain an arm-type site equivalent in location to *P′3* in KplE1, and we showed in this paper that this site is the most dispensable in integrative as well as in excisive recombination. A possible explanation is that this site was originally present in P4 and disappeared, whereas it is still present in KplE1. This may be due to the defective nature of the KplE1 prophage that has a fixed genome as it is not able to replicate independently of the host genome. However, the fact that HK620, Sf6 and CUS-3 phages share the same module organization than KplE1 rules out the fixed genome hypothesis. Phage P2 has an even more simplistic *att*L organization with only two arm-type binding sites (Fig. 1B), which suggests that the same sites are used to assemble the excisive as well as the integrative intasome. Thus, our results reinforce the idea that the intasome assembly is specific to the recombination module that is considered, since the composition and the orientation of the recombination regions vary from one module to another.

Materials and methods

Strain construction

Strain LCB984 is a derivative of strain MC4100 (Casadaban, 1976) and was constructed by the insertion of the *kan* gene in the KplE1 prophage between *yfdO* and *yfdP* according to the method of Datsenko and Wanner (2000). The presence of the *kan* gene was verified by PCR amplification of the chromosomal region (the sequence of the primers is available upon request to the authors). Strains LCB6022 (*hupA hupB*), LCB6023 (*hns*), LCB6027 (*fis*), and LCB6028 (*ihfA*) are derivative of strain MC4100. Appropriate mutations of nucleoid associated protein (NAP) genes from the KEIO collection (Baba et al., 2006) were introduced by P1 transduction into strain MC4100. The resulting strains were then transformed with plasmid PCP20 that encodes the λ flippase (FLP) (Datsenko and Wanner, 2000). Thermal induction of the flippase gene in these strains allowed the removal of the *kan* gene that is flanked by two FRT sites. Finally, P1 lysate prepared from strain LCB984 (KplE1 Kan^R) was used to transduce the Kan^R marker into strains mutated for the various NAP genes.

In vivo excision assay

Strains LCB6022 (*hupA hupB*), LCB6023 (*hns*), LCB6027 (*fis*), and LCB6028 (*ihfA*) carrying *torI* encoding plasmid pJFi (Ansaldi et al., 2004) were grown in LB medium until the OD600 reached 0.5 units, and IPTG (1 mM) was added for 2 h at 37 °C under agitation. Control cells were grown under the same conditions except that no IPTG was added to the cultures. Appropriate culture dilutions were plated onto rich medium containing either 25 μg mL^{-1} ampicillin or 12.5 μg mL^{-1} kanamycin. Numeration of the CFU plated on both antibiotics was performed and the ratio of ampicillin-resistant/kanamycin-resistant colonies was calculated. Values represent the average of at least three independent determinations.

Mutagenesis and preparation of DNA substrates

To generate DNA fragments mutated on *O*, *P*, *P′*, *I* and *H* sites, two different strategies were used. When the mutagenesis site was close to the end of the DNA fragment, the mutation was included directly in the PCR primer. When the mutagenesis site was far from the end of the DNA fragment, we performed a 2-step PCR reaction with overlapping intermediate PCR products bearing the mutation. For all sites, 4 to 5 conserved base pairs were changed to the complement: GGGGA was changed to CCCCT in *O* sites; TAAA was changed to ATTT in *P* and *P′* sites, GTTCG, GTCCG and GATCG were changed to CAAGC in all *I* sites, and ATCA was changed to TAGT in *H* sites. All primer sequences are available upon request. Resulting PCR products were all cloned into the pCR2.1 vector (Invitrogen) and sequence accuracy was checked by sequencing. Substrates for band-shift assays were produced using 5′-Cy5 labeled primers (Eurogentec) at one extremity.

Protein purifications

IntS, TorI and IHF proteins were overproduced and purified near homogeneity using their DNA binding (Heparin column) and basic (SP column) properties as described (Ansaldi et al., 2004; Panis et al., 2007; Murtin et al., 1998). The purity of TorI, IntS and IHF was estimated by running the purified fractions onto a 20% SDS–Tris/Tricine–PAGE followed by Coomassie blue staining. The absence of contamination of TorI and IntS preparations by IHF was checked by Western blot using IHF antisera. The protein concentrations were estimated by the Lowry method.

In vitro integration and excision assays

In vitro reactions were performed as described (Panis et al., 2007). Briefly, all reaction mixtures (25 µl) included linear *att* sites mutated or non-mutated (32 nM) in buffer containing 20 mM Tris–HCl (pH 7.4), 50 mM KCl, 10 mM spermidine, 5 mM EDTA, 1 mg mL^{-1} bovine serum albumin, and 5% glycerol. Protein concentrations were optimized to the use of linear DNA substrates, therefore IHF (0.25 µM), IntS (0.8 µM), and TorI (1.6 µM) were added as indicated in the figure legends. The reactions were carried out in optimized conditions: 37 °C for 1 h at an IHF:IntS:TorI protein ratio of 1:3:6. The abundance of *att*P formed during *in vitro* excision assays (*att*L and *att*R substrates) and the abundance of *att*R formed during *in vitro* integration assays (*att*B and *att*P substrates) were quantified by real-time PCR as described (Panis et al., 2007) on a Mastercycler ep realplex (Eppendorf) using the SYBR Premix Ex Taq™ kit (TaKaRa) according to the manufacturer recommendations.

Band shift assays

Reaction mixes (20 µL) contained Cy5 labeled DNA (100 nM) in 40 mM Tris–HCl pH 7.6 buffer containing 2.5 mg mL^{-1} sonicated calf thymus DNA, 1 mg mL^{-1} BSA, 100 mM KCl and 10% glycerol. Appropriate protein concentrations indicated in figure legends were added prior to incubation at 25 °C for 30 min. Samples were loaded on a 4% native PAGE pre-ran 30 min in TBE 1× at 90 V, and ran for 3 more hours at 135 V. Migration profiles were then analyzed by scanning the gel using a 635 nm laser and a LPR filter (FLA5100, Fujifilm).

DNAse I footprinting assay

Primer attL-ter was labeled with [γ-^{32}P]ATP (4000 Ci $mmol^{-1}$) using T4 polynucleotide kinase (Promega, Madison, WI). The labeled primer was separated from unincorporated [γ-^{32}P]ATP by using the Nucleotide Removal Kit (Qiagen). *att*L DNA fragment was PCR-amplified by using MC4100 chromosomal DNA as a template with appropriate labeled and unlabeled primers (attL-pro/attL-ter). The footprint assays were performed as follows: the labeled DNA fragment was diluted to a concentration of ~1 nM in 50 µl of binding mix (10 mM Tris–HCl, pH 7.5, 50 mM NaCl, 2.5 mM $MgCl_2$, 0.5 mM dithiothreitol, 4% glycerol, and 40 ng $µl^{-1}$ poly(dI–dC)·poly(dI–dC)) to which different amounts of purified IntS and/or TorI were added. After 30 min of incubation at room temperature, DNase I was added (0.07 unit, Invitrogen), and the reaction was conducted for 1 min, then stopped by the addition of 140 µl of DNase Stop Solution (192 mM sodium acetate, 32 mM EDTA, 0.14% SDS, and 64 µg ml^{-1} yeast RNA). After DNA ethanol-precipitation in the presence of a DNA carrier (Pellet Paint co-precipitant, Novagen), the pellets were resuspended in a loading dye solution (95% formamide, 10 mM EDTA, 0.3% bromophenol blue, 0.3% xylene cyanol) and loaded onto a 8% polyacrylamide/6 M urea electrophoresis gel. The locations of the protected nucleotides were deduced by running a ladder with products of the G+A cleavage reaction according to Maxam and Gilbert.

Cross-linking analysis

20 µM IntS or 100 µM TorI was incubated 15 min at 25 °C in the presence or absence of the homobifunctional sulhydryl reactive agent bis(maleimido)hexane (BMH, 1 mM, Pierce). *att*L DNA (222 bp, 100 nM) was also added to the reaction when indicated. Samples were ran on a 7% (IntS) or 7–16% (TorI) Tricine–SDS PAGE. The proteins were either revealed by Coomassie blue staining (IntS) or transferred onto a nitrocellulose membrane and revealed by immunodetection with specific antisera.

Size exclusion chromatography

500 µL of IntS (20 µM) was loaded onto a Superdex™ 200 (GE Healthcare) previously calibrated with appropriate protein markers and the elution profile at 280 nm was recorded.

Acknowledgments

We would like to thank C. Bourges for technical assistance in mutagenesis and Marie-Thérèse Giudici-Orticoni for her help with size exclusion chromatography. We also thank T. Mignot and T. Puvirajesinghe for the critical reading of the manuscript. This work was supported by the Centre National de la Recherche Scientifique and grant JC05_41524 from the Agence Nationale pour la Recherche (ANR) to MA. GP is a fellowship recipient from the French Research Ministry (MENRT).

References

Abbani, M.A., Papagiannis, C.V., Sam, M.D., Cascio, D., Johnson, R.C., Clubb, R.T., 2007. Structure of the cooperative Xis–DNA complex reveals a micronucleoprotein filament that regulates phage lambda intasome assembly. Proc. Natl. Acad. Sci. U. S. A 104, 2109–2114.

Abremski, K., Gottesman, S., 1981. Site-specific recombination Xis-independent excisive recombination of bacteriophage lambda. J. Mol. Biol. 153, 67–78.

Abremski, K., Gottesman, S., 1982. Purification of the bacteriophage lambda *xis* gene product required for lambda excisive recombination. J. Biol. Chem. 257, 9658–9662.

Ahlgren-Berg, A., Cardoso-Palacios, C., Eriksson, J.M., Mandali, S., Sehlen, W., Sylwan, L., Haggard-Ljungquist, E., 2009. A comparative analysis of the bifunctional Cox proteins of two heteroimmune P2-like phages with different host integration sites. Virology 385, 303–312.

Ansaldi, M., Théraulaz, L., Méjean, V., 2004. TorI, a response regulator inhibitor of phage origin in *Escherichia coli*. Proc. Natl. Acad. Sci. U. S. A 101, 9423–9428.

Argos, P., Landy, A., Abremski, K., Egan, J.B., Haggard-Ljungquist, E., Hoess, R.H., Kahn, M. L., Kalionis, B., Narayana, S.V., Pierson III, L.S., 1986. The integrase family of site-specific recombinases: regional similarities and global diversity. EMBO J. 5, 433–440.

Baba, T., Ara, T., Hasegawa, M., Takai, Y., Okumura, Y., Baba, M., Datsenko, K.A., Tomita, M., Wanner, B.L., Mori, H., 2006. Construction of *Escherichia coli* K-12 in-frame, single-gene knockout mutants: the Keio collection. Mol. Syst. Biol. 2, 2006.

Ball, C.A., Johnson, R.C., 1991. Efficient excision of phage lambda from the Escherichia coli chromosome requires the Fis protein. J. Bacteriol. 173, 4027–4031.

Biswas, T., Aihara, H., Radman-Livaja, M., Filman, D., Landy, A., Ellenberger, T., 2005. A structural basis for allosteric control of DNA recombination by lambda integrase. Nature 435, 1059–1066.

Cali, S., Spoldi, E., Piazzolla, D., Dodd, I.B., Forti, F., Deho, G., Ghisotti, D., 2004. Bacteriophage P4 Vis protein is needed for prophage excision. Virology 322, 82–92.

Casadaban, M.J., 1976. Transposition and fusion of the lac genes to selected promoters in *Escherichia coli* using bacteriophage lambda and Mu. J. Mol. Biol. 104, 541–555.

Casjens, S., 2003. Prophages and bacterial genomics: what have we learned so far? Mol. Microbiol. 49, 277–300.

Casjens, S., Winn-Stapley, D.A., Gilcrease, E.B., Morona, R., Kuhlewein, C., Chua, J.E., Manning, P.A., Inwood, W., Clark, A.J., 2004. The chromosome of *Shigella flexneri* bacteriophage Sf6: complete nucleotide sequence, genetic mosaicism, and DNA packaging. J. Mol. Biol. 339, 379–394.

Cho, E.H., Nam, C.E., Alcaraz Jr., R., Gardner, J.F., 1999. Site-specific recombination of bacteriophage P22 does not require integration host factor. J. Bacteriol. 181, 4245–4249.

Clark, A.J., Inwood, W., Cloutier, T., Dhillon, T.S., 2001. Nucleotide sequence of coliphage HK620 and the evolution of lambdoid phages. J. Mol. Biol. 311, 657–679.

Datsenko, K.A., Wanner, B.L., 2000. One-step inactivation of chromosomal genes in *Escherichia coli* K-12 using PCR products. Proc. Natl. Acad. Sci. U. S. A 97, 6640–6645.

ElAntak, L., Ansaldi, M., Guerlesquin, F., Méjean, V., Morelli, X., 2005. Structural and genetic analyses reveal a key role in prophage excision for the TorI response regulator inhibitor. J. Biol. Chem. 280, 36802–36808.

Fadeev, E.A., Sam, M.D., Clubb, R.T., 2009. NMR structure of the amino-terminal domain of the lambda integrase protein in complex with DNA: immobilization of a flexible tail facilitates beta-sheet recognition of the major groove. J. Mol. Biol. 388, 682–690.

Frumerie, C., Sylwan, L., Ahlgren-Berg, A., Haggard-Ljungquist, E., 2005. Cooperative interactions between bacteriophage P2 integrase and its accessory factors IHF and Cox. Virology 332, 284–294.

Gardner, J.F., Nash, H.A., 1986. Role of *Escherichia coli* IHF protein in lambda site-specific recombination. A mutational analysis of binding sites. J. Mol. Biol. 191, 181–189.

Goodman, S.D., Kay, O., 1999. Replacement of integration host factor protein-induced DNA bending by flexible regions of DNA. J. Biol. Chem. 274, 37004–37011.

Goodman, S.D., Nicholson, S.C., Nash, H.A., 1992. Deformation of DNA during site-specific recombination of bacteriophage lambda: replacement of IHF protein by HU protein or sequence-directed bends. Proc. Natl. Acad. Sci. U. S. A 89, 11910–11914.

Gottesman, S., Abremski, K., 1980. The role of HimA and Xis in lambda site-specific recombination. J. Mol. Biol. 138, 503–512.

Hazelbaker, D., Azaro, M.A., Landy, A., 2008. A biotin interference assay highlights two different asymmetric interaction profiles for lambda integrase arm-type binding sites in integrative versus excisive recombination. J. Biol. Chem. 283, 12402–12414.
Huang, W., Yuan, C., Ansaldi, M., Morelli, X., Meehan, E.J., Chen, L.Q., Huang, M., 2007. Expression, purification, crystallization and molecular replacement studies of TorI, an inhibition protein of Tor system. Chin. J. Struct. Chem. 26, 594–598.
Jessop, L., Bankhead, T., Wong, D., Segall, A.M., 2000. The amino terminus of bacteriophage lambda integrase is involved in protein–protein interactions during recombination. J. Bacteriol. 182, 1024–1034.
Kamadurai, H.B., Foster, M.P., 2007. DNA recognition via mutual-induced fit by the core-binding domain of bacteriophage lambda integrase. Biochemistry 46, 13939–13947.
King, M.R., Vimr, R.P., Steenbergen, S.M., Spanjaard, L., Plunkett III, G., Blattner, F.R., Vimr, E.R., 2007. *Escherichia coli* K1-specific bacteriophage CUS-3 distribution and function in phase-variable capsular polysialic acid O acetylation. J. Bacteriol. 189, 6447–6456.
Kovach, M.J., Tirumalai, R., Landy, A., 2002. Site-specific photo-cross-linking between lambda integrase and its DNA recombination target. J. Biol. Chem. 277, 14530–14538.
Lee, S.Y., Radman-Livaja, M., Warren, D., Aihara, H., Ellenberger, T., Landy, A., 2005. Non-equivalent interactions between amino-terminal domains of neighboring lambda integrase protomers direct Holliday junction resolution. J. Mol. Biol. 345, 475–485.
Lewis, J.A., Hatfull, G.F., 2001. Control of directionality in integrase-mediated recombination: examination of recombination directionality factors (RDFs) including Xis and Cox proteins. Nucleic Acids Res. 29, 2205–2216.
Miller, H.I., Friedman, D.I., 1980. An *E. coli* gene product required for lambda site-specific recombination. Cell 20, 711–719.
Miller, H.I., Mozola, M.A., Friedman, D.I., 1980. int-h: an *int* mutation of phage lambda that enhances site-specific recombination. Cell 20, 721–729.
Murtin, C., Engelhorn, M., Geiselmann, J., Boccard, F., 1998. A quantitative UV laser footprinting analysis of the interaction of IHF with specific binding sites: re-evaluation of the effective concentration of IHF in the cell. J. Mol. Biol. 284, 949–961.
Nash, H.A., Robertson, C.A., 1981. Purification and properties of the *Escherichia coli* protein factor required for lambda integrative recombination. J. Biol. Chem. 256, 9246–9253.
Numrych, T.E., Gumport, R.I., Gardner, J.F., 1991. A genetic analysis of Xis and FIS interactions with their binding sites in bacteriophage lambda. J. Bacteriol. 173, 5954–5963.
Numrych, T.E., Gumport, R.I., Gardner, J.F., 1992. Characterization of the bacteriophage lambda excisionase (Xis) protein: the C-terminus is required for Xis-integrase cooperativity but not for DNA binding. EMBO J. 11, 3797–3806.
Nunes-Duby, S.E., Kwon, H.J., Tirumalai, R.S., Ellenberger, T., Landy, A., 1998. Similarities and differences among 105 members of the Int family of site-specific recombinases. Nucleic Acids Res. 26, 391–406.
Panis, G., Méjean, V., Ansaldi, M., 2007. Control and regulation of KplE1 prophage site-specific recombination: a new recombination module analyzed. J. Biol. Chem. 282, 21798–21809.
Papagiannis, C.V., Sam, M.D., Abbani, M.A., Yoo, D., Cascio, D., Clubb, R.T., Johnson, R.C., 2007. Fis targets assembly of the Xis nucleoprotein filament to promote excisive recombination by phage lambda. J. Mol. Biol. 367, 328–343.
Radman-Livaja, M., Biswas, T., Ellenberger, T., Landy, A., Aihara, H., 2006. DNA arms do the legwork to ensure the directionality of lambda site-specific recombination. Curr. Opin. Struct. Biol. 16, 42–50.
Rice, P.A., Yang, S., Mizuuchi, K., Nash, H.A., 1996. Crystal structure of an IHF–DNA complex: a protein-induced DNA U-turn. Cell 87, 1295–1306.
Rudd, K.E., 1999. Novel intergenic repeats of *Escherichia coli* K-12. Res. Microbiol. 150, 653–664.
Sam, M.D., Papagiannis, C.V., Connolly, K.M., Corselli, L., Iwahara, J., Lee, J., Phillips, M., Wojciak, J.M., Johnson, R.C., Clubb, R.T., 2002. Regulation of directionality in bacteriophage lambda site-specific recombination: structure of the Xis protein. J. Mol. Biol. 324, 791–805.
Shiga, Y., Sekine, Y., Kano, Y., Ohtsubo, E., 2001. Involvement of H-NS in transpositional recombination mediated by IS1. J. Bacteriol. 183, 2476–2484.
Smith, M.C., Thorpe, H.M., 2002. Diversity in the serine recombinases. Mol. Microbiol. 44, 299–307.
Thompson, J.F., Waechter-Brulla, D., Gumport, R.I., Gardner, J.F., Moitoso de Vargas, L., Landy, A., 1986. Mutations in an integration host factor-binding site: effect on lambda site-specific recombination and regulatory implications. J. Bacteriol. 168, 1343–1351.
Tirumalai, R.S., Healey, E., Landy, A., 1997. The catalytic domain of lambda site-specific recombinase. Proc. Natl. Acad. Sci. U. S. A 94, 6104–6109.
Tirumalai, R.S., Kwon, H.J., Cardente, E.H., Ellenberger, T., Landy, A., 1998. Recognition of core-type DNA sites by lambda integrase. J. Mol. Biol. 279, 513–527.
Yu, A., Haggard-Ljungquist, E., 1993. The Cox protein is a modulator of directionality in bacteriophage P2 site-specific recombination. J. Bacteriol. 175, 7848–7855.